

Hydrogen Adsorption in an Interpenetrated Dynamic Metal–Organic Framework

Banglin Chen,^{*,†} Shengqian Ma,[‡] Fatima Zapata,[†] Emil B. Lobkovsky,[§] and Jun Yang^{||}

Department of Chemistry, University of Texas-Pan American, Edinburg, Texas 78541-2999,
Department of Chemistry and Biochemistry, Miami University, Oxford, Ohio 45056,
Baker Laboratory, Department of Chemistry and Chemical Biology, Cornell University,
Ithaca, New York 14853-1301, and Department of Chemistry, University of Michigan,
Ann Arbor, Michigan 48109-1055

Received March 14, 2006

A metal–organic framework $\text{Zn}(\text{NDC})(4,4'\text{-Bpe})_{0.5} \cdot x\text{G}$ [NDC = 2,6-naphthalenedicarboxylate; 4,4'-Bpe = 4,4'-*trans*-bis(4-pyridyl)-ethylene; G = guest molecules] has been synthesized, structurally characterized, and rationalized to be a two-interpenetrated elongated primitive cubic net. Powder X-ray diffraction and adsorption studies reveal the dynamic feature of the framework, which can take up hydrogen of about 2.0 wt % at 77 K and 40 bar and 0.3 wt % at 298 K and 65 bar.

Porous metal–organic frameworks (MOFs) have been emerging as one type of the most promising materials for hydrogen storage because of their amenability to design and extraordinary permanent porosity.^{1,2} To maximize the hydrogen packing within the pores and to enhance the interactions of hydrogen molecules with porous MOFs, it has been a daunting challenge to reach the target goal of hydrogen storage of 9.0 wt % in 2015 for FreedomCAR economy, specified by the Department of Energy.³ Current efforts have been mainly focused on robust MOFs to rationalize the factors such as porosity, catenation, and open metal sites for hydrogen uptake,^{4–16} while the potential use of dynamic MOFs for hydrogen storage has been rarely realized.^{8b,18}

Recently, Kim,⁷ Hupp,^{17a} and ourselves^{8b} have been particularly interested in pillared paddle-wheel frameworks for their functional properties and dynamic features of framework interpenetration. Our recently reported microporous MOF $\text{Zn}(\text{BDC})(4,4'\text{-Bipy})_{0.5}$, exhibiting dynamic open–dense framework transformations and 1D pores of about $4.0 \times 4.0 \text{ \AA}$ to discriminate linear and branched alkanes, has been successfully applied to the gas chromatographic separation of alkanes.^{8b} Herein we report a rare example of dynamic MOF $\text{Zn}(\text{NDC})(4,4'\text{-Bpe})_{0.5} \cdot 2.25\text{DMF} \cdot 0.5\text{H}_2\text{O}$ [**1**; NDC = 2,6-

* To whom correspondence should be addressed. E-mail: banglin@utpa.edu.

[†] University of Texas-Pan American.

[‡] Miami University.

[§] Cornell University.

^{||} University of Michigan.

- (1) Yaghi, O. M.; O'Keeffe, M.; Ockwig, N. W.; Chae, H. K.; Eddaoudi, M.; Kim, J. *Nature* **2003**, *423*, 705. Férey, G.; Mellot-Draznié, C.; Serre, C.; Millange, F. *Acc. Chem. Res.* **2005**, *38*, 217.
- (2) Chae, H. K.; Siberio-Pérez, D. Y.; Kim, J.; Go, Y. B.; Eddaoudi, M.; Matzger, A. J.; O'Keeffe, M.; Yaghi, O. M. *Nature* **2004**, *427*, 523. Férey, G.; Mellot-Draznié, C.; Serre, C.; Millange, F.; Dutour, J.; Surlé, S.; Margiolaki, I. *Science* **2005**, *309*, 2040.
- (3) Hydrogen, Fuel Cells & Infrastructure Technologies Program: Multi-year Research, Development, and Demonstration Plan. U.S. Department of Energy, 2005, <http://www.eere.energy.gov/hydrogenandfuelcells/mypp/>.
- (4) Millange, F.; Serre, C.; Férey, G. *Chem. Commun.* **2002**, 822. Férey, G.; Latroche, M.; Serre, C.; Millange, F.; Loiseau, T.; Percheron-Guegan, A. *Chem. Commun.* **2003**, 2976.

- (5) (a) Rowsell, J. L. C.; Yaghi, O. M. *Angew. Chem., Int. Ed.* **2005**, *44*, 4670. (b) Rowsell, J. L. C.; Yaghi, O. M. *J. Am. Chem. Soc.* **2006**, *128*, 1304. (c) Wong-Foy, A. G.; Matzger, A. J.; Yaghi, O. M. *J. Am. Chem. Soc.* **2006**, *128*, 3494.
- (6) Pan, L.; Sander, M. B.; Huang, X.; Li, J.; Smith, M. R., Jr.; Bittner, E. W.; Bockrath, B. C.; Johnson, J. K. *J. Am. Chem. Soc.* **2004**, *126*, 1308. Lee, J. Y.; Pan, L.; Kelly, S. P.; Jagiello, J.; Emge, T. J.; Li, J. *Adv. Mater.* **2005**, *17*, 2703.
- (7) Dybtsev, D. N.; Chun, H.; Kim, K. *Angew. Chem., Int. Ed.* **2004**, *43*, 5033. Chun, H.; Dybtsev, D. N.; Kim, H.; Kim, K. *Chem.—Eur. J.* **2005**, *11*, 3521.
- (8) (a) Chen, B.; Ockwig, N. W.; Millward, A. R.; Contreras, D. S.; Yaghi, O. M. *Angew. Chem., Int. Ed.* **2005**, *44*, 4745. (b) Chen, B.; Liang, C.; Yang, J.; Contreras, D. S.; Clancy, Y. L.; Lobkovsky, E. B.; Yaghi, O. M.; Dai, S. *Angew. Chem., Int. Ed.* **2006**, *45*, 1390.
- (9) Kesanli, B.; Cui, Y.; Smith, M. R., Jr.; Bittner, E. W.; Bockrath, B. C.; Lin, W. *Angew. Chem., Int. Ed.* **2005**, *44*, 72.
- (10) Lee, E. Y.; Suh, M. P. *Angew. Chem., Int. Ed.* **2004**, *43*, 2798. Lee, E. Y.; Jang, S. Y.; Suh, M. P. *J. Am. Chem. Soc.* **2005**, *127*, 6374.
- (11) (a) Kaye, S. S.; Long, J. R. *J. Am. Chem. Soc.* **2005**, *127*, 6505. (b) Dinca, M.; Long, J. R. *J. Am. Chem. Soc.* **2005**, *127*, 9376.
- (12) Sun, D.; Ke, Y.; Mattox, T. M.; Ooro, B. A.; Zhou, H.-C. *Chem. Commun.* **2005**, 5447. Sun, D.; Ma, S.; Ke, Y.; Collins, D. J.; Zhou, H.-C. *J. Am. Chem. Soc.* **2006**, *128*, 3896.
- (13) Zhao, X.; Xiao, B.; Fletcher, A. J.; Thomas, K. M.; Bradshaw, D.; Roesseinsky, M. J. *Science* **2004**, *306*, 1012.
- (14) (a) Dietzel, P. D. C.; Panella, B.; Hirscher, M.; Blom, R.; Fjellvag, H. *Chem. Commun.* **2006**, 959. (b) Panella, B.; Hirscher, M.; Putter, H.; Muller, U. *Adv. Funct. Mater.* **2006**, *16*, 520.
- (15) Dailly, A.; Vajo, J. J.; Ahn, C. C. *J. Phys. Chem. B* **2006**, *110*, 1099.
- (16) (a) Li, Y.; Yang, R. T. *J. Am. Chem. Soc.* **2006**, *128*, 726. (b) Li, Y.; Yang, R. T. *J. Am. Chem. Soc.* **2006**, ASAP.
- (17) (a) Ma, B.-Q.; Mulfort, K. L.; Hupp, J. T. *Inorg. Chem.* **2005**, *44*, 4912. (b) Choi, E.-Y.; Park, K.; Yang, C.-M.; Kim, H.; Son, J.-H.; Lee, S. W.; Lee, Y. H.; Min, D.; Kwon, Y.-U. *Chem.—Eur. J.* **2004**, *10*, 5535.
- (18) Kitagawa, S.; Kitaura, R.; Noro, S. *Angew. Chem., Int. Ed.* **2004**, *43*, 2334. Uemura, K.; Matsuda, R.; Kitagawa, S. *J. Solid State Chem.* **2005**, *178*, 2420.

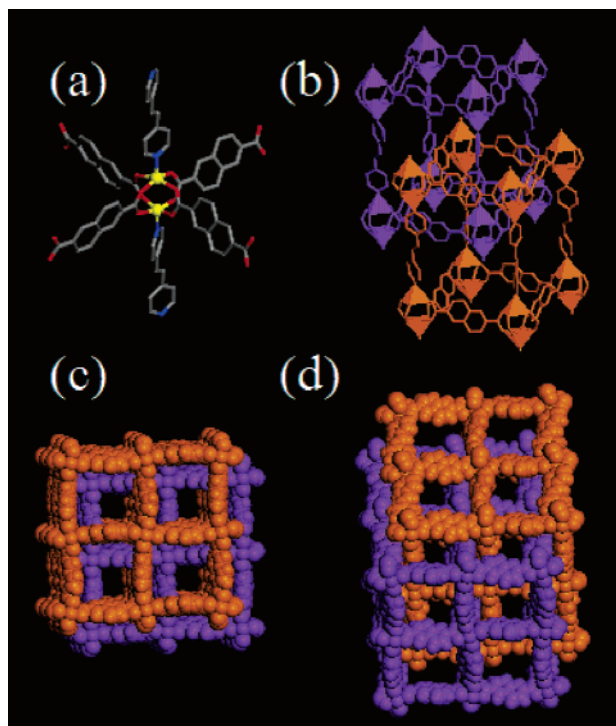


Figure 1. X-ray crystal structure of MOF **1** showing (a) the coordination geometry of the paddle-wheel $\text{Zn}_2(\text{NDC})_2(4,4'\text{-Bpe})$ unit (H atoms are omitted for clarity; Zn, yellow; N, blue; O, red; C, gray), (b) two interpenetrated primitive cubic nets, and space-filling representations of (c) a 1D channel of $5.1 \times 6.0 \text{ \AA}$ along the a axis and (d) a 1D channel of $4.3 \times 4.3 \text{ \AA}$ viewed along the rectangular diagonal of the paddle-wheel clusters.

naphthalenedicarboxylate; 4,4'-Bpe = 4,4'-*trans*-bis(4-pyridyl)ethylene; DMF = *N,N*-dimethylformamide] of two interpenetrated primitive cubic nets for hydrogen storage.

MOF **1** was synthesized by the solvothermal reaction of H_2NDC , 4,4'-Bpe, and $\text{Zn}(\text{NO}_3)_2 \cdot 6\text{H}_2\text{O}$ in DMF at 100°C for 24 h as colorless block-shaped crystals.¹⁹ It was formulated as $\text{Zn}(\text{NDC})(4,4'\text{-Bpe})_{0.5} \cdot 2.25\text{DMF} \cdot 0.5\text{H}_2\text{O}$ by elemental microanalysis and single-crystal X-ray diffraction studies,²⁰ and the phase purity of the bulk material was independently confirmed by powder X-ray diffraction (PXRD) and thermal gravimetric analysis (TGA).

As expected, the framework is composed of paddle-wheel dinuclear Zn_2 units (Figure 1a), which are bridged by NDC dianions and further pillared by 4,4'-Bpe to form a 3D two-interpenetrated elongated primitive cubic (α -Po) structure (Figure 1b). Because of double interpenetration of the 3D frameworks, the pores of MOF **1** are reduced to ca. $5.1 \times 6.0 \text{ \AA}$ along the a axis (Figure 1c) and ca. $4.3 \times 4.3 \text{ \AA}$ along the rectangular diagonal of the paddle-wheel clusters (Figure

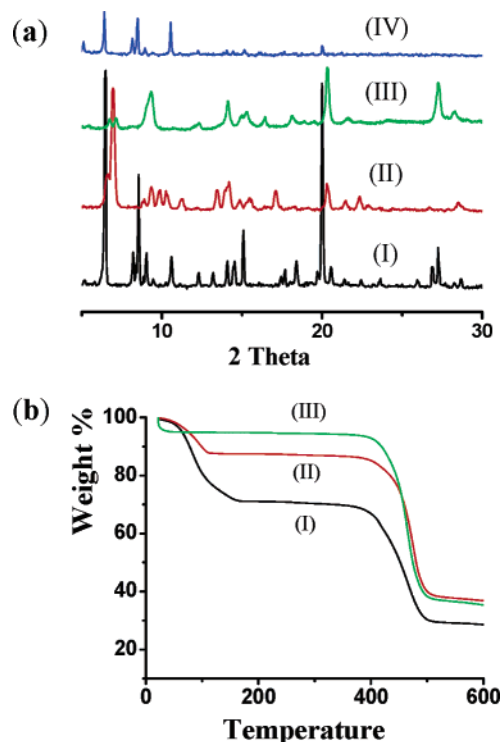


Figure 2. (a) XPRD patterns of as-synthesized (I, black), acetone-exchanged (II, red), methanol-exchanged (III, green), and regenerated (IV, blue) MOF **1** and (b) TGA traces of as-synthesized (I, black), acetone-exchanged (II, red), and methanol-exchanged (III, green) MOF **1**.

1d). Because both organic linkers of NDC and 4,4'-Bpe in MOF **1** are longer than those of BDC and 4,4'-Bipy in MOF $\text{Zn}(\text{BDC})(4,4'\text{-Bipy})_{0.5}$, the pores in MOF **1** are much larger than the 1D pores of $4.0 \times 4.0 \text{ \AA}$ in $\text{Zn}(\text{BDC})(4,4'\text{-Bipy})_{0.5}$.^{8b}

Because there exist no specific interactions between the two interpenetrated frameworks, MOF **1** was expected to exhibit the dynamic feature involving framework transformations/deformations as revealed in MOF $\text{Zn}(\text{BDC})(4,4'\text{-Bipy})_{0.5}$.^{8b} Immersion of the as-synthesized MOF **1** in pure acetone led to the reduced d spacing of the structure, as shown in the acetone-exchanged PXRD pattern (Figure 2a, II, red), which was systematically right shifted, while immersion of the as-synthesized MOF **1** in pure methanol immediately led to the cracking of the single crystals and produced a completely different PXRD pattern (Figure 2a, III, green). Such a significant change of PXRD patterns might be attributed to the guest-induced framework squeezes because of the flexibility of the 4,4'-Bpe ligand, forming less porous MOFs.¹⁸ The as-synthesized MOF **1** has larger pores than those exchanged with acetone and methanol molecules to accommodate solvent molecules; thus, the framework squeezes are also partially responsible for their different TGA behaviors in which the as-synthesized MOF **1** liberated more guest molecules (Figure 2b, I, black) than the acetone-exchanged (Figure 2b, II, red) and methanol-exchanged (Figure 2b, III, green) MOF **1** did. Soaking methanol-exchanged MOF **1** in DMF for 1 day regenerated the as-synthesized MOF **1** whose PXRD pattern matches quite well with that of the as-synthesized MOF **1** (Figure 2a, IV, blue); therefore, the framework transformations are reversible.

(19) MOF **1**: A mixture of $\text{Zn}(\text{NO}_3)_2 \cdot 6\text{H}_2\text{O}$ (0.438 g, 1.47 mmol), H_2NDC (0.318 g, 1.47 mmol), and 4,4'-Bpe (0.134 g, 0.74 mmol) was suspended in DMF (60 mL) and heated in a vial (60 mL) at 100°C for 24 h. The colorless block-shaped crystals formed were collected, washed with DMF and hexane, and dried in air (0.62 g, 75%). Elem anal. Calcd for $\text{Zn}(\text{NDC})(4,4'\text{-Bpe})_{0.5} \cdot 2.25\text{DMF} \cdot 0.5\text{H}_2\text{O}$ ($\text{C}_{24.75}\text{H}_{27.75}\text{N}_{3.25}\text{O}_{6.75}\text{Zn}$): C, 54.63; H, 5.14; N, 8.36. Found: C, 54.92; H, 4.78; N, 8.09.

(20) Crystal data for MOF **1**: $\text{Zn}_2(\text{NDC})_2(4,4'\text{-Bpe}) \cdot 5\text{DMF} \cdot \text{H}_2\text{O}$, monoclinic, space group $P2(1)/c$, $a = 16.1578(5) \text{ \AA}$, $b = 18.8070(6) \text{ \AA}$, $c = 18.1039(5) \text{ \AA}$, $\beta = 92.6150(10)^\circ$, $V = 5495.7(3) \text{ \AA}^3$, $Z = 4$, $D_{\text{calc}} = 1.357 \text{ g/cm}^3$, $\mu = 0.941 \text{ mm}^{-1}$, $T = 173 \text{ K}$, $R1 [I > 2\sigma(I)] = 0.0477$, $wR2$ (all data) = 0.1564, $S = 1.048$.

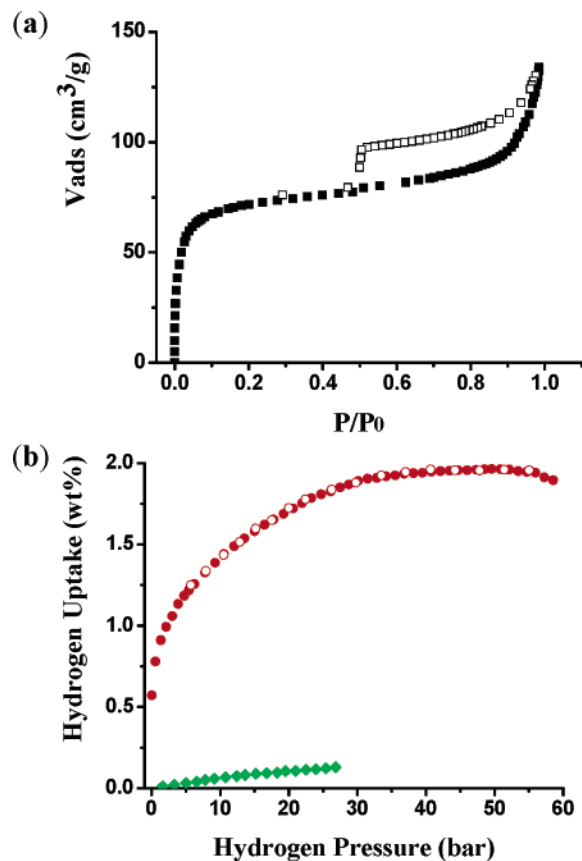


Figure 3. (a) Nitrogen sorption isotherm at 77 K and (b) high-pressure hydrogen isotherm for activated MOF **1** at 77 K (red) and 298 K (green).

To examine permanent porosity, methanol-exchanged MOF **1** was activated at a temperature of 150 °C under vacuum overnight for gas sorption studies. The nitrogen sorption isotherm (Figure 3a) shows typical type I sorption behavior with a Langmuir surface area (A_s) of 303 m²/g and a pore volume of 0.20 cm³/g. The surface area is significantly low for such a highly porous crystal structure and is only about one-third of 946 m²/g for MOF Zn(BDC)(4,4'-Bipy)_{0.5}.^{8b} In fact, it is even lower than the three-interpenetrated cobalt analogy Co(NDC)(4,4'-Bpe)_{0.5} of 484 m²/g.^{17b} Obviously, the pores in activated MOF **1** have not been fully expanded in 1 atm of nitrogen, and the nitrogen adsorption is not saturated. The nitrogen sorption displays hysteretic sorption behavior because of the dynamic feature of the frameworks.^{8b,18}

A high-pressure hydrogen isotherm was carried out using an automated controlled Sieverts' apparatus (Hy-Energy LLC) over a pressure range of 0–60 bar. The hydrogen adsorption isotherms of MOF **1** measured at 77 K and room temperature are shown in Figure 3. At 77 K, the sorption

isotherm has a type I profile, saturated at 40 bar with a hydrogen uptake of about 2.0 wt %. Adsorption and desorption processes for physisorption of hydrogen molecules in MOF **1** are fully reversible. It is worth noting that a high-pressure hydrogen uptake of 2.0 wt % in MOF **1** is comparable to those found in MOF-74 of 2.3 wt %^{5c} and Ni₂(DHTP) of 1.8 wt %^{14a} with surface areas of 1070 and 1083 m²/g, respectively. The volumetric hydrogen storage is 18 g/L at 77 K and 40 bar. Such a high hydrogen uptake is attributed to the full usage of the pores in MOF **1** at higher pressures. The room-temperature hydrogen storage capacity is expected to be about 0.3 wt % at 65 bar, which is comparable to those found in MOF-5 of 0.28 wt % with a high surface area of 2296 m²/g.^{14b} The hydrogen uptakes are reproducible. After sorption studies, the framework recovered back to the initially activated one under vacuum, as shown in their XPRD patterns. To the best of our knowledge, MOF **1** is the highest hydrogen storage dynamic MOF material at 77 K, although the uptake is quite lower than the highest one of 7.5 wt % for MOF-177 at 77 K and 70 bar.^{5c}

The high hydrogen uptake in MOF **1** at moderate pressures reveals the potential use of dynamic MOF materials for high-pressure hydrogen storage. As was recently rationalized, huge porosity of robust MOFs will be the prerequisite for high hydrogen storage at low temperature and high pressure.^{5c} We suspect that dynamic MOFs with huge structural porosity might also be good candidates for hydrogen storage and need to be further examined, although their permanent porosity might be low because of framework transformations/deformations. The pursuit for high hydrogen storage MOF materials at room temperature will be much more challenging and the future endeavor will be focused on implementation of specific hydrogen sorption sites to maximize their hydrogen uptake.¹⁶

Acknowledgment. This work was supported by the University of Texas-Pan American (UTPA) through a Faculty Research Council award (B.C), in part by the Welch Foundation (Grant BG-0017) to the Department of Chemistry at UTPA. We thank Drs. Alexandra N. Torgersen and Anne Dailly at GM for their generous help with the high-pressure hydrogen sorption studies and Dr. Omar M. Yaghi and Dr. Hong-Cai Zhou for the access to their facilities. The reviewer's comments on the framework dynamic feature are greatly appreciated.

Supporting Information Available: X-ray data in CIF format, PXRD patterns, and sorption data. This material is available free of charge via the Internet at <http://pubs.acs.org>.

IC060437T